R-spondin3 is associated with basal-progenitor behavior in normal and tumor mammary cells

AUTHORS AND AFFILIATIONS: Johanna M. Tocci[1], Carla M. Felcher[1]; Martín E. García Solá[1], María Victoria Goddio[1], María Noel Zimberlin[1], Natalia Rubinstein[1,2], Anabella Srebrow[1,2], Omar A. Coso[1,2], Martín C. Abba[3], Roberto P. Meiss[4], Edith C. Kordon[1,5]§

1. CONICET-Universidad de Buenos Aires, Instituto de Fisiología, Biología Molecular y Neurociencias (IFIBYNE), Buenos Aires, Argentina.

2. Universidad de Buenos Aires, Facultad de Ciencias Exactas y Naturales, Departamento de Fisiología, Biología Molecular y Celular, Buenos Aires, Argentina.

3. Basic and Applied Immunological Research Center, School of Medicine, National University of La Plata, Argentina.

4. Department of Pathology, Institute of Oncology Studies, National Academy of Medicine, Buenos Aires, Argentina.

5. Universidad de Buenos Aires, Facultad de Ciencias Exactas y Naturales, Departamento de Química Biológica, Buenos Aires, Argentina.

§Corresponding author: Edith Claudia Kordon. IFIBYNE-UBA-CONICET, Ciudad Universitaria, 1428 Ciudad Autónoma de Buenos Aires, Argentina. e-mail: ekordon@qb.fcen.uba.ar

RUNNING TITLE: RSPO3 promotes basal-like behavior in mammary cells

The authors declare no competing financial interests.

ABBREVIATIONS: BCCL, breast cancer cell line; CSC, cancer stem cell; CM, conditioned media; KD, Knock-down; MaSC, mammary stem cell; MMTV, mouse mammary tumor virus; rRSPO3, recombinant R-spondin3; TCGA, the cancer genome atlas; TN, triple-negative.

WORD COUNT: 5496 (excluding Figure legends and References).

Abstract

R-spondin3 (RSPO3) is a member of a family of secreted proteins that enhance Wnt signaling pathways in diverse processes including cancer. However, the role of RSPO3 in mammary gland and breast cancer development remains unclear. In this study, we show that RSPO3 is expressed in the basal stem cell-enriched compartment of normal mouse mammary glands but is absent from committed mature luminal cells in which exogenous RSPO3 impairs lactogenic differentiation. RSPO3 knockdown in basal-like mouse mammary tumor cells reduced canonical Wnt signaling, epithelial-to-mesenchymal transition-like features, migration capacity, and tumor formation *in vivo*. Conversely, RSPO3 overexpression, which was associated with some LGR and RUNX factors, highly correlated with the basal-like subtype among breast cancer patients. Thus we identified RSPO3 as a novel key modulator of breast cancer development and a potential target for treatment of basal-like breast cancers.

Introduction

R-spondins (*roof plate-specific spondins;* RSPOs) represent a group of four secreted proteins (RSPO1–4) that have been described in vertebrates. All four RSPOs have similar domain structures with two amino-terminal furin-like repeats and a thrombospondin domain situated towards the basic amino acid-rich carboxyl terminal domain which can bind matrix glycosaminoglycans and/or proteoglycans [1]. RSPOs potently enhance both canonical, through β-catenin activation, and non-canonical *Wnt* signaling pathways [2-4]. At the cell membrane, secreted RSPOs simultaneously bind to leucine-rich repeat-containing G-protein coupled receptors 4, 5 or 6 (LGR4-6) [5, 6], and to extracellular domains of two membrane-bound E3 ubiquitin ligases, Zinc and RING finger 3/RING finger 43 (ZNRF3/RNF43). This ternary complex, LGR-RSPO-ZNRF3/RNF43, induces auto-ubiquitination and membrane clearance of ZNRF3/RNF43, allowing the WNT receptor, Frizzled (FZD), to accumulate and enhance the activation of *Wnt* pathways [7].

WNT ligands activate canonical *Wnt* signaling by binding to FZD receptor, inducing the release of β-catenin from a cytosolic destruction multi-protein complex and its translocation to the nucleus where it acts as a co-activator of the TCF/LEF family of transcription factors, promoting target gene transcription. This signaling pathway is essential to several developmental processes by regulation of cell proliferation, differentiation, and migration, whilst its de-regulation underlies a wide range of pathologies including cancer [8].

The mammary gland undergoes most of its development postnatally, progressing through a series of developmental cycles regulated by systemic hormones and local factors [9, 10]. The mammary epithelium is composed by luminal and basal compartments, surrounded by adipocytes and other stromal cells. The basal compartment consists of myoepithelial cells with contractile capacity and WNT-responsive mammary stem cells (MaSCs) [11] that reconstitute the gland upon transplantation into cleared mammary fat pads of host syngeneic mice [12]. Importantly, LGRs have been recently described as MaSC markers and are WNT-regulated target genes [13, 14]. Moreover, canonical *Wnt* signaling plays a critical role in controlling the enormous tissue expansion and remodeling during mammary gland development [15] through the maintenance and differentiation of MaSCs [16], and is implicated in breast carcinogenesis [17].

Due to their *Wnt* pathway-potentiating activity, RSPOs play critical roles in embryonic development and organogenesis as well as in the self-renewal and maintenance of stem cells in some adult tissues [1]. Likewise, genomic rearrangements and transcriptional activation that result in elevated RSPO expression have been recently identified in mouse and human tumors, suggesting RSPOs may be functionally relevant for tumor development [18-20]. Particularly, RSPO3 promotes angio- and vasculogenesis [21, 22], several steps during embryogenesis [4], and represents a potent intestinal stem cell factor [23]. Acting through canonical and non-

canonical *Wnt* pathway activation, RSPO3 has been recently implicated in several cancer models including colorectal, ovarian, and lung cancer [24, 25].

Several years ago, mouse mammary tumor virus (MMTV) insertions that promoted *Rspo3* overexpression were identified [26, 27]. However, the role of RSPO3 in breast cancer and normal mammary gland development remains unclear. Here, we show that RSPO3 is expressed in the basal stem cell-enriched compartment of the mouse mammary gland. In mammary tumor cells its overexpression is associated with the maintenance of mesenchymal-like features, migration capacity and *in vivo* tumorigenesis. Moreover, we found that RSPO3 is associated with the basal-like human breast cancer subtype, which lacks efficient therapeutic options.

Materials and methods

Cell culture, transfections, and differentiation procedures

The following mouse mammary cell lines, obtained directly from their originating laboratories or from American Type Culture Collection (ATCC), were used in this study: HC11 and EpH4 (Dr. Bernd Groner; Georg-Speyer-Haus), LM3 (Dr. Elisa Bal; Institute of Oncology Ángel H. Roffo), NMuMG (ATCC), SCg6 and SCp2 (Dr. Mina Bissell; Lawrence Berkeley National Laboratory), and LM38-LP (Dr. Laura Todaro; Institute of Oncology Ángel H. Roffo) [28]. Since no mouse STR DNA fingerprinting analysis is available for them to date, no authentication was performed (see Supplementary Material for culture and differentiation procedures). SCg6 cells were stably transfected with pGIPZ/tGFP/shScrambled/Puromycin or with different shRNA sequences of pGIPZ/tGFP/shRSPO3/Puromycin (Thermo-Scientific), and resistant clones were selected with 2 µg/ml puromycin (Sigma-Aldrich) for 4 weeks. For epithelial-to-mesenchymal transition (EMT) assay, NMuMG cells were incubated with 60 ng/ml recombinant RSPO3 protein (rRSPO3; R&D) or 2 ng/ml TGFβ (Sigma-Aldrich) at indicated times. All cell lines used in this study were maintained in culture for 4 to 5 weeks, regularly monitored for mycoplasma contamination by PCR using specific primers and discarded in case of positive results.

RT-qPCR

Total RNA was isolated using TriReagent (MRC) according to the manufacturer's instructions. For RT, 250 ng or 1 µg RNA from sorted mouse mammary cell populations or cell cultures, respectively, were used. All qPCRs were performed using SYBR Green (Roche) and Stratagene Mx3000P System (Agilent-Technologies). Gene expression levels were normalized to *Actinb1*, *Gapdh* or *Hsp90ab1* as reference genes using standard curve method. See Supplementary Material for more details and primer sequences.

Protein analysis

Total proteins were extracted in RIPA buffer and used for Western blotting (WB). Blocked membranes were incubated with primary and secondary antibodies as follows: pAKT and AKT (Cell-Signaling; 4060S and 9272, respectively), E-cadherin (Thermo-Scientific; 13-1900; ECCD2 clone), p-JNK, JNK, β-Actin and GAPDH (SCBT; sc-6254, sc-474, sc-1616 and sc-20357, respectively), RSPO3 (R&D Systems; MAB41201), Vimentin (Abcam; 7783-500), IgG anti-mouse, anti-rabbit, or anti-rat (SCBT; sc-2005, sc-2004, and sc-2032, respectively). More details in Supplementary Material.

Conditioned media

To obtain conditioned media (CM), cells were cultured in supplemented medium for 24 h that was replaced with serum-free medium for another 24 h or 48 h, as indicated. CMs were collected, precipitated overnight at -20°C with acetone, and centrifuged at 1500g and 4°C for 20 min. Pellets were resuspended in 40 µl PBS containing

SDS sample buffer and used for WB. For competitive assay, cells were incubated with increasing concentrations of $KClO_3$ (Sigma-Aldrich) in serum-free medium prior CM collection.

Wound healing assay

Confluent monolayers were wounded with a pipette tip, cell debris was removed by washing with warm medium and cells were cultured for 15 h in serum-free medium. Images were captured using an Olympus SP-350 digital camera mounted on a microscope after wounding (t=0h) and 15 h later. Analysis was performed using Image-Pro-Plus software and wound sizes in experimental monolayers were expressed relatively to controls.

β-catenin transcriptional activity

Cells were transfected with 1 µg/well of pGL3-OT (TOP-Flash-like, TCF-LEF/β-catenin reporter), and pCMVLacZ as a control. Transfections were performed using Polyethylenimine (Polysciences) according to manufacturer's instructions. Cell extracts were prepared 48 h or 72 h later, using Reporter Lysis Buffer (Promega). Luciferase pGL3-OT activity was normalized to pCMVLacZ β-galactosidase activity. See Supplementary Material for detailed data.

Immunofluorescence

Fixed cells or 5-µm paraffin sections of mammary glands from 12-week-old mice were incubated with F-actin probe Rhodamine Phalloidin (Sigma-Aldrich), anti-αSMA (Abcam, ab21027), anti-β-catenin (BD; #610154), anti-ERα (SCBT; sc-542), anti-Fibronectin (Sigma; F6140; clone FN-3E2), anti-RSPO3 (Sigma-Aldrich; HPA029957) or anti-Vimentin (Abcam; 7783-500) antibodies followed by incubation with Alexa Fluor 555 goat anti–mouse IgG, 647 donkey anti–mouse IgG, 488 donkey anti-goat IgG, and 647 donkey anti–rabbit IgG (Life-Technologies). Cells were also stained with DAPI (Roche). Slides were examined under an Olympus FV100 confocal microscope and images were analyzed with MacBiophotonics ImageJ. See Supplementary Material for more details.

Animals

Virgin female mice from C57BL/6 and BALB/c strains were maintained in a specific pathogen–free facility at the FCEN-UBA-CONICET, at constant temperature and humidity with a 12 h light cycle. Animals were allowed food and water *ad libitum*. Mouse experiments were approved by local IACUC authorities and complied with regulatory standards of animal ethics.

Cell isolation and fluorescence-activated cell sorting

Lymph node-free mammary glands from 12-week-old virgin C57BL/6 mice were minced and digested to obtain single-cell suspensions prior flow cytometry analysis. See Supplementary Material for more details. For FACS, 5×10^5 cells from mouse single-cell suspensions were stained with fluorophore-conjugated antibodies (BioLegend). Specifically, cells were stained with anti-mouse CD31/CD140a/TER119/CD45-PE (Lineage cocktail; clones 145-2C11, RB6-8C5, M1/70, RA3-6B2 and Ter-119), anti-hamster IgG/anti-rat IgG2b/anti-rat IgG2a as lineage cocktail isotype controls, anti-mouse CD24-APC (clone M1/69) or anti-mouse CD29-FITC, for 30 min on ice in 10% (v/v) FBS/PBS. Stained populations were analyzed and sorted on a BD FACS Aria (II) Cell Sorting System (BD). Data acquisition and analysis were performed using FACS Diva software (BD).

***In vivo* studies**

Six-week-old virgin BALB/c female mice were injected subcutaneously into the right ventral flank or within the right 4^{th} mammary fat pad with 4×10^5 SCg6-shRspo3 or SCg6-shControl cells in 100 µl DMEM-F12 (8 mice per group; n=3). Alternatively, 20-day-old BALB/c female mice were subjected to standard mammary fat pad clearing and then injected with the same amount of the indicated cells within the #4 cleared fat pads. Tumor measurements

were carried out blindly with a caliper twice per week, and volumes were calculated using the formula $V=\pi/6\times length\times(width)^2$. Mice were euthanized when they met the institutional criteria for tumor size and overall health condition. Tumors were fixed in PBS-buffered 4% (v/v) formalin solution and embedded in paraffin. Lung experimental metastasis was induced by injecting 7×10^5 cells in 100 µl PBS through the tail vein. Up to 4 weeks post-injection, animals were euthanized and their lungs were fixed via tracheal instillation of 4% (v/v) buffered formalin prior to removal. Paraffin-embedded lung samples were stained with H&E and entirely scanned. Metastatic regions in H&E-stained lungs were quantified by a metastasis area index, calculated as the ratio of metastasis to total lung areas.

Immunohistochemistry

Immunohistochemistry (IHC) analysis were performed on 5-µm paraffin sections either of mammary glands from 12-week-old mice, mouse tumors and lungs samples, or human mammary tissues with the Vectastain Elite ABC HRP Kit (Vector-Laboratories) according to the manufacturer's instructions. Primary antibodies used were as follows: αSMA (Thermo-Fisher-Scientific, #RB-9010), cleaved-caspase3 (CC3) (Cell-Signaling; 9661), ERα (SCBT; sc-542), Ki67 (Abcam; ab15580), KRT-14 (Thermo-Fisher-Scientific; #RB-9020), RSPO3 (Sigma-Aldrich; HPA029957), SOX2 (Cell-Signaling; 3728) or Vimentin (Abcam; 7783-500). For CC3 and Ki67 quantification, cells were counted at 1000X (5 fields per section at least; 1000 cells per field) excluding boundaries and necrotic regions; n=3.

Human mammary tissues

Tissue microarray (TMA) of breast cancers was purchased from US Biomax (#BR1505b). Paraffin-embedded breast tissue specimens were acquired from hospitals associated to the School of Medical Sciences - National University of La Plata, after obtaining written informed consents from patients (according to Declaration of Helsinki, 2000) and the approval by the Institutional Review Board.

***In silico* analysis**

Comparative analysis of *RSPO3, CDH1*, *FN1*, *VIM*, *SNAI1*, *SNAI2* and *TWIST* gene expression was performed in 51 breast normal and cancer cell lines obtained from three independent studies (GSE10843, GSE12777 and GSE41445). Expression profiles were developed using the Affymetrix HG-U133 Plus2 platform (GPL570). Mouse *Rspo3* mRNA expression was analyzed among luminal cells isolated from the mammary glands of adult female mice derived from the GSE47377 dataset obtained from GEO2R resource. Visualization and statistical analysis of RSPO3 expression were done with R/Bioconductor. Comparative analysis of *RSPO3*, *LGR4-6*, *RUNX1-3* mRNA expression profiles across 1097 primary human breast carcinomas was performed using The Cancer Genome Atlas (TCGA) Network, breast cancer project. Correlation analysis was done with Pearson's test using corrplot R package. Profiles were also compared according to PAM50-intrinsic subtypes and ESTIMATE (Estimation of STromal and Immune cells in Malignant Tumors using Expression data) scores. Comparative analysis of *RSPO3*, *ER*/*PR*/*HER2* and *CDH1/VIM/SNAI2/TWIST* mRNA expression among 1985 breast cancer samples was done using the METABRIC dataset. Kruskal-Wallis and Chi-squared were used as statistic tests. See Supplementary Material for more details.

Statistical methods

Statistical significance of differences was evaluated using the software GraphPad Prism5 (La Jolla, CA, USA). Data are presented as mean ± s.e.m unless otherwise noted.

Results

RSPO3 is expressed in distinct mouse and human mammary cell lines

In order to assess whether *Rspo3* is expressed in mammary cells in the absence of MMTV infection, we performed an *in silico RSPO3* mRNA profiling analysis in a set of 51 human breast normal and cancer cell lines. Obtained values revealed that breast cancer cells express high levels of *RSPO3* as compared to the non-tumorigenic cell line MCF-10A. Interestingly, among tumor cells, *RSPO3* mRNA levels resulted higher in basal-like (ER^-PR^-) than in luminal-like (ER^+PR^+) breast cancer cell lines (BCCLs). Notably, a subset of basal ER^-PR^- cells (i.e., MDA-MB-436, HCC1143, BT549, HDQP1, and Hs578t), which are characterized by low expression of epithelial cell-cell adhesion and luminal differentiation markers, as well as by high expression of genes involved in EMT and cancer stem cell (CSC) features [29], showed the highest level of *RSPO3* expression (Figure 1A, 1B and S1). Besides, we determined a significant correlation of *RSPO3* with some of those markers, as *CDH1*, *VIM* and *TWIST1* (Figure 1C and D). In addition, analysis of mouse mammary tumors also revealed that ER^- cells (LM38-LP and SCg6) express higher levels of *Rspo3* than ER^+ tumor cells (C4 derived, MPA-induced tumors, see Supplementary Material) (Figure 1E). Among non-tumor cell lines (HC11, EpH4 and SCp2), we found that *Rspo3* mRNA levels were associated with vimentin expression, a broadly used basal/mesenchymal marker, and that proliferating HC11 cells showed the highest *Rspo3* levels (Figure 1E). This cell line produces its own extracellular matrix and resembles mammary stem/progenitor cells in the proliferating undifferentiated stage, exhibiting pluripotent capacity and expression of proteins associated to mesenchymal phenotype [30]. Importantly, as these cells reached lactogenic differentiation, *Rspo3* expression significantly decreased, similarly to vimentin levels (Figure 1E).

At the protein level, it was determined that RSPO3 is secreted to the extracellular space, as it was detected in the CM of cultured mammary tumor cells (Figure 1F). Our results also confirmed that, once secreted, RSPO3 may strongly interact with membrane-associated and/or extracellular matrix heparan sulfate proteoglycans, since the addition of potassium chlorate, an inhibitor of sulfation, increased RSPO3 levels in the CM of mammary tumor cells (Figure 1G).

RSPO3 is differentially expressed in stromal and basal mammary subpopulations

To determine whether RSPO3 is constitutively expressed in the normal mouse mammary gland, studies using IHC were carried out. RSPO3 cytoplasmic staining was detected in a subset of basal epithelial cells and within the stroma. Figure 2A shows its localization as well as the distribution of basal myo-epithelial markers cytokeratin 14 (KRT14) and α-smooth-muscle actin (α-SMA), and the MaSC marker SOX2 [14] on serial mammary sections. Noteworthy, RSPO3 localization was clearly different from the luminal marker, estrogen receptor-α (ERα) (Figure 2A and B) and co-immunofluorescent studies also revealed accumulation of RSPO3 surrounding α-SMA positive cells (Figure 2B).

To identify the specific subpopulations expressing *Rspo3*, we examined its mRNA level in FACS-purified luminal ($Lin^-CD24^{hi}CD29^+$), MaSC-enriched basal ($Lin^-CD24^+CD29^{hi}$) epithelial and stromal ($Lin^-CD24^-CD29^+$) populations (Figure 2C). The successful separation was confirmed by *Krt18* (luminal), *Krt14* (basal) and *Vim* (basal/stromal) marker expression analysis (Figure 2D). We found that *Rspo3* was predominantly expressed in stromal cells and in the MaSC-enriched basal epithelial fraction. Interestingly, in the mammary epithelial compartment, we observed that *Rspo3* levels displayed a similar distribution as its putative receptor, the basal MaSC marker, *Lgr4* [14] (Figure 2D). Collectively, these data demonstrate that RSPO3 is expressed in normal mammary glands of adult virgin female mice both in the stem cell-enriched basal epithelial and stromal populations, whereas it is absent from committed luminal epithelial cells.

RSPO3 is associated with basal phenotype in mammary cells

As indicated above (Fig. 1E), *Rspo3* levels decrease as HC11 cells reach lactogenic differentiation in culture. In addition, *in silico* analysis revealed that the committed alveolar luminal cell population of mid-pregnant animals expresses lower levels of *Rspo3* than alveolar luminal stem/progenitor mammary cells of virgin mice (Figure 3A). Moreover, we determined that recombinant RSPO3 (rRSPO3) protein significantly reduced β-casein expression levels in luminal-like, functionally normal SCp2 and EpH4 cells under lactogenic conditions (Figure 3B). To further investigate whether RSPO3 could alter mammary epithelial phenotype, we cultured NMuMG cells with rRSPO3 protein. It was observed that rRSPO3 induced canonical Wnt pathway activation (Figure S2A) and promoted the acquisition of fibroblast-like, mesenchymal morphology, similar to that obtained with transforming growth factor-β (TGF-β) (Figure 3C). We detected a significantly increased expression of the mesenchymal markers fibronectin and vimentin, and a reduced expression of the epithelial marker E-cadherin by RT-qPCR and/or WB analysis (Figure 3D and E). Similar results were obtained in SCp2 cells after rRSPO3 treatment (Figure S2B). Taken together, these results suggest that RSPO3 could play a relevant role in the normal mammary gland biology, promoting the maintenance of an uncommitted basal-like mammary epithelial phenotype and inducing EMT-like and CSC features, which may be the underlying mechanisms for transforming breast cancer cells that overexpress RSPO3.

To validate the involvement of RSPO3 in the malignant phenotype of basal cancer cells, the SCg6 cell line, which expresses high levels of *Rspo3* (Fig. 1E), was stably transfected with a scrambled shRNA (shControl) or with four different *Rspo3* shRNA sequences. Two clones (#2A and #4B) displaying a knock-down (KD) efficiency of ~50% at mRNA and protein levels were selected for further studies (Figures 4A and S3A). Rspo3-KD cells showed a change in cell morphology from spread-out, mesenchymal-like to cobble-stone, epithelial-like cells when cultured up to confluence (Figure 4B). Although subtler, cell shape differences were also detected at sub-confluence (Figure S3B). Consistently, F-actin was predominantly reorganized into cortical bundles associated with cell-cell adhesions in Rspo3-KD cells in contrast to the F-actin assembled into thick parallel bundles, or actin stress fibers, in shControl cells (Figure 4C). Moreover, an increase in membrane-bound β-catenin levels, as a key component of cell–cell adhesion, was obtained in Rspo3-KD cells as compared to stabilized-cytoplasmic β-catenin displayed by shControl cells (Figure 4D). Although E-cadherin expression remained undetectable, analysis of basal/mesenchymal markers revealed a reduction of vimentin and fibronectin levels in Rspo3-KD cells, as compared to shControl cells (Figure 4E and F). We also determined that the morphological change observed in Rspo3-KD cells was accompanied by a significant decrease in migration capacity (Figure 4G).

Then, we investigated the signaling pathway underlying RSPO3 activity in tumor basal mammary cells. While no changes in JNK phosphorylation levels were found (Figure S3C), as a non-canonical *Wnt* pathway activation marker, Rspo3-KD cells displayed a significant reduction of canonical *Wnt* pathway activation, since less nuclear β-catenin activity was detected by reporter gene expression (Figure 4H). In addition, Rspo3-KD cells exhibited a reduction in AKT phosphorylation levels (Figure S3D), in agreement with several reports showing the role of phosphoinositide 3-kinase (PI3K)/AKT pathway in enhancing canonical *Wnt* pathway during normal mammary gland development and tumorigenesis [31]. Taken together, these results suggest that RSPO3 could be relevant for breast cancer progression favoring the maintenance of a migratory basal/mesenchymal-like phenotype possibly through canonical *Wnt* pathway activation and a crosstalk with the PI3K/AKT cascade.

***Rspo3*-KD reduces *in vivo* tumor growth and metastasis in basal mammary cancer cells**

To determine the effect of knocking-down *Rspo3* on tumor growth *in vivo*, Rspo3-KD and shControl SCg6 cells were subcutaneously injected into female mice. It was determined that shControl-derived tumors appeared earlier

and grew faster than those obtained from Rspo3-KD cells. Nine days after cell injection all shControl-derived tumors were palpable and had to be euthanized 20 days after injection due to their tumor size. In contrast, tumors from Rspo3-KD cells appeared much later, or did not show tumor development even after 60 days post-inoculation (Figure 5A). A similar study was performed inoculating parental, shControl and Rspo3-KD SCg6 cells into the #4 mammary fat pads, up to 20 days post-injection to compare tumors at the same end-point. Once again, tumors from Rspo3-KD cells arose later and were smaller than those derived from control cells (Figures 5B and C). Histological analysis revealed that both Rspo3-KD and shControl tumors expressed RSPO3 and were composed by undifferentiated spindle cells that invaded mammary fat tissue and entrapped host mammary ducts (Figure S4). In addition, when Rspo3-KD and shControl cells were transplanted into cleared fat pads, no differences to the previous approaches regarding tumor growth were detected. After 9 days shControl tumors reached 69.9±23.3 mm^3 and displayed invasive behavior towards the fatty stroma, while Rspo3-KD-derived tumors were barely palpable and looked encapsulated (H&E staining, Figure 5D). Besides, Rspo3-KD implants displayed heterogeneous lower expression of RSPO3 and Vimentin, as well as less Ki67 positive nuclei and a higher number of Cleaved-Caspase3 (CC3) positive cells, compared to shControl tumors (Figure 5D).

To determine whether RSPO3 also affects secondary tissue invasion, Rspo3-KD and shControl cells were injected into the tail vein of female mice. Fifteen days after injection, mice carrying shControl cells exhibited lung micro-metastasis, which fully developed into macro-metastasis that comprised the entire lungs two weeks later. In contrast, no tumor tissue was observed in lungs of mice carrying Rspo3-KD cells 15 days post-inoculum, and in only one of them a single macro-metastasis was found 30 days after injection (Figure 5E). Besides, sequentially sliced lungs of mice inoculated with Rspo3-KD cells showed a significant reduction in the number of micro-metastasis compared to controls (Figure 5F and G). All together, these data demonstrate the relevance of RSPO3 for *in vivo* development of a basal mammary tumor model.

RSPO3 is overexpressed in human breast cancer and is associated with basal-like tumors

In order to assess *RSPO3* expression in human mammary tissue, IHC was performed on 21 samples of malignant and benign breast lesions. We found that most of these samples showed positive immunoreactivity for RSPO3 (62%; 13/21) (Figures 6 A-D and Table S1). Furthermore, RSPO3 was clearly detected in the basal compartment of differentiated ducts and lobules in neoplastic and non-neoplastic samples (Figures 6 E-H). RSPO3 expression was then analyzed by IHC in a TMA of 74 invasive ductal breast carcinoma cases. Notably, 70% (52/74) of tumors showed low to strong RSPO3 positive staining, while only 30% (22/74) resulted negative (z-test: $p<0.001$; Figure 6I-N). When RSPO3-score was compared with clinical and histopathological parameters, neither clinical stage nor biomarker (ER/PR/Her2 and Ki67) expression exhibited a significant correlation with RSPO3 levels (Tables S2-4). However, the expression data of the TCGA-Breast cancer project from 1985 human breast carcinomas, revealed that *RSPO3* was highly expressed in triple-negative (TN) samples ($ER^-PR^-Her2^-$) compared to ER^+ subtypes ($ER^+PR^{+/-}Her2^{+/-}$) (Figure 7A), and showed significant *RSPO3* overexpression in the basal-like subtype (Figure 7B). Moreover, by sub-dividing basal-like breast cancer category within the intrinsic subtypes, we determined significantly high *RSPO3* expression in claudin-low, basal-like tumors (Figure 7C), which are characterized by low to absent expression of differentiated luminal cell markers, high enrichment for EMT markers, immune response genes, and CSC-like features [29]. Besides, *RSPO3* mRNA levels were negatively correlated with epithelial markers, as E-cadherin, and positively with the EMT and CSC markers, vimentin, *SLUG* and *TWIST,* in primary human breast tumors (Figure 7D). Then, through the ESTIMATE method, we found that *RSPO3* expression was associated with elevated lymphocytic and stromal components (Figure 7E), which are present in most basal-like breast cancers [32]. Nevertheless, no significant association between *RSPO3* mRNA expression and lower overall survival was detected in patients with basal-like primary breast carcinomas (Figure S5A).

Finally, to propose RSPO3 as a relevant autocrine breast tumor factor, we analyze expression levels of certain factors previously shown to promote RSPOs expression and activity. *In silico* analysis revealed that among breast carcinomas *RSPO3* is expressed in association with the three RSPOs receptors, *LGR4-6* (Figure 7F), and showed a positive correlation with the runt-related transcription factor (RUNX) family (Figure S5B) that may induce *Rspo3* expression in mammary tumor cells [33]. Particularly, *RSPO3* levels significantly correlated with *LGR4-6* and *RUNX3* levels, among the members of these two families (Figure 7G). Comparisons between different intrinsic molecular breast cancer subtypes revealed that these genes were also overexpressed in the basal-like subtype (Figure 7H), consistently with *RSPO3* expression.

Discussion

Activation of *Wnt* pathway has been described as a cell-biological program required for the correct development of the mammary gland [15], particularly promoting the maintenance and differentiation of MaSCs [16]. RSPOs and LGR4–6 were recently found to constitute a ligand-receptor system with critical roles in normal development and stem cell survival through modulation of *Wnt* signaling in several tissues [5, 6]. However, their roles in breast carcinogenesis have been less explored. Previously, we identified MMTV-promoted *Rspo3* up-regulation [26], which led to mammary tumor formation in mice [27]. We have also observed that 3T3 cells overexpressing *Rspo3* showed cell contact inhibition and anchorage-independent growth, which confirmed its pro-oncogenic capacity, as well as modulation of AKT and JNK signaling pathways (Figure S6, A-D).

Here, we show that *RSPO3* is overexpressed in human BCCLs compared to non-tumor cells. Interestingly, the highest levels of *RSPO3* mRNA were found in a subset of basal-like BCCLs with a highly aggressive phenotype and EMT and CSC features [34]. Consistently, established basal-like mouse mammary cell lines that exhibited high *Rspo3* levels also expressed vimentin, a basal/mesenchymal marker described as a target of canonical *Wnt* pathway activation promoting cell migration and invasion in human breast cells [35]. The association between *Rspo3* and vimentin was also evident in the non-tumorigenic mammary cell line HC11, since detectable levels of both mRNAs were found in the proliferative phase. Interestingly, proliferative-undifferentiated HC11 cells are considered stem-like cells due to their self-renewal and pluripotent capacity [30]. In agreement with these observations, we determined that in mice *Rspo3* is expressed by the basal, stem cell-enriched mouse mammary compartment, associated with the expression of the RSPOs' receptor, *Lgr4*. Likewise, RSPO3 was detected in the basal layer of neoplastic and non-neoplastic ducts in human glands. Thus, these findings suggest that RSPO3 might be playing a relevant role in *Wnt* pathway activation and MaSCs maintenance. A similar role of RSPO3 has been described in the intestinal stem niche, where it enhances the activity of WNT ligands secreted by epithelial and stromal populations [23]. In fact, inhibition of RSPO3 activity, using blocking antibodies in human colorectal tumor xenographs, reduces the expression of several tumor stem cell-associated genes, thereby linking the activity of RSPO3 to the maintenance of epithelial homeostasis and the tumorigenesis of that tissue through hyperactivation of stem cell genes [25]. In addition, we showed that RSPO3, once secreted, remains bound to the extracellular matrix and/or face of the cell membrane, and therefore it may exert its activity on the same cell population. Moreover, we found that *Rspo3* expression decreased as HC11 cells reach lactogenic differentiation, whereas rRSPO3 reduced β-casein expression in differentiated luminal cells. Hence, our results suggest that RSPO3 would participate in maintaining the stem niche of the normal mammary gland, inhibiting differentiation of the luminal compartment.

We are not the first to find out that a member of the RSPO protein family is present in the normal mouse mammary gland. It has been demonstrated that *Rspo1* is expressed by luminal cells and, together with WNT4,

mediates hormone action on mammary stem cell expansion [36]. We still do not know whether *Rspo3* expression in the gland is regulated during development. However, its presence in stromal and basal mammary cells suggests that RSPO3 would contribute to the maintenance of the MaSCs and/or the MaSC niche in the adult female mice, since it has been shown a similar distribution and biological role in the intestine [23]. Moreover, as *RSPO1* mRNA levels resulted lower than *RSPO3* in basal-like breast cancers (Figure 7B and S7), we propose that RSPO3 would play a more significant role in the development of this breast cancer subtype.

Many extracellular factors and signaling pathways described in normal mammary gland development and tumorigenesis, such as the canonical *Wnt* pathway, are also involved in the process of EMT [37-39]. In this study, we observed that RSPO3 caused the acquisition of a spindle-shaped phenotype, typical of cells that have lost their epithelial properties, together with the modulation of relevant EMT markers. Interestingly, it has been determined that certain features associated with a partial EMT are visible in non-tumor conditions, playing an important role in adult tissue remodeling. For example, during normal mammary branching morphogenesis, EMT-related genes are expressed specifically in terminal end buds, inhibiting epithelial differentiation in favor of the acquisition of migratory features [40, 41]. Therefore, the ability of RSPO3 to induce EMT-associated events might also be important for mammary gland development during puberty.

Our results also demonstrate that RSPO3 is relevant for the migratory basal/mesenchymal-like phenotype in mouse mammary tumor cells, possibly through canonical *Wnt* pathway activation and a crosstalk with the PI3K/AKT cascade. This conclusion is based on the following obtained evidences: (1) RSPO3 promoted the maintenance of a spindle-shaped morphology and the expression of CSC- and EMT-associated genes such as vimentin and fibronectin; (2) RSPO3 increased the ability of basal tumor cells to migrate in culture and to grow and invade secondary tissues *in vivo*; (3) RSPO3 enhances canonical *Wnt* pathway activation and AKT phosphorylation, interplay also observed by our group in *Rspo3*-overexpressing 3T3 cells. Collectively, these results are consistent with reports showing that canonical *Wnt* signaling blockage decreases migratory potential and growth in soft-agar of basal-like breast cancer cells [42, 43] and that the crosstalk between β-catenin/*Wnt* and PI3K/AKT pathways plays a critical role in the regulation of normal and malignant stem/progenitor cells during mammary gland development and carcinogenesis [44, 45]. Besides, our *in silico* analysis shows that *RSPO3* mRNA levels were associated with high expression of stem cell markers in tumors from breast cancer patients. Therefore, RSPO3 might promote the transcription of stem cell-related genes during normal and neoplastic mammary development through activation of *Wnt*/AKT pathways. The long latency of shRspo3-SCg6 tumors indicates the relevance of this protein for *in vivo* tumor development. Since Claudin-low breast tumor cells show high expression of RSPO3, and this cancer subtype has been shown to be enriched in functional CSCs [46], we postulate that inhibiting expression of RSPO3 in SCg6 cells may decrease their cancer stem properties, reducing the capability of tumor grafting and growth *in vivo*. Therefore, the impact of altering RSPO3 levels on Wnt pathway activation, EMT and migration capacity observed in culture would be associated to SCg6-cancer stem cell population ability for survival, grafting and generation of the appropriate microenvironment for tumor implantation and development *in vivo*.

By IHC, we found that most tumor samples from 74 breast cancer patients resulted positive for RSPO3, while no significant association between this protein and the levels of clinically relevant biomarkers was determined. However, RNA-Seq analysis of 1985 human breast carcinomas from the TCGA-Breast cancer database revealed that *RSPO3* was highly expressed in TN samples, compared to ER^+ tumors, independently from their PR and Her2 levels, and in the basal-like subtype among the intrinsic categories [29]. This cancer subtype is a heterogeneous breast cancer group with less therapeutic options than luminal tumors, since they lack ER/PR expression and $Her2/Neu^+$ amplification. Several studies have recently demonstrated a high cytoplasmic and

nuclear accumulation of β-catenin in ~60% of human breast cancers, particularly in TNs, associated with the expression of EMT-related genes [47] and a MaSC enrichment [48-50]. These results, beyond relating canonical *Wnt* pathway with a poor clinical prognosis, showed that this activation was not due to mutations in β-catenin gene, highlighting the importance of studying new factors, as RSPO3, that could enhance canonical *Wnt* pathway activation in the most aggressive forms of breast cancer. Interestingly, we determined a positive association of *RSPO3* with *LGR4-6* and *RUNX3*, which are also over-represented in the basal subtype. Although a dual activity of *RUNX* genes in promoting or inhibiting breast cancer development has been established [51], the data shown herein are consistent with our recent report showing that RUNX1 activates the transcription of *Rspo3* in mouse mammary tumor cells [33]. Therefore, we propose that deregulation of the RUNX family might also lead to *RSPO3* overexpression in human breast cancer. However, further studies will be required to dissect the exact mechanism of how the RUNX3-RSPO3-LGR axis functions to modulate *Wnt* signaling in TN breast cancers.

Within the basal category, we found a significant higher expression of *RSPO3* in the claudin-low subtype. It has been shown that in both mice and humans, this subtype has the largest percentage of tumors in which the MaSC signature predominates [52]. However, given that these aggressive tumors exhibit EMT and CSCs features [29], they may originate from the luminal progenitor population prior to acquiring adult MaSC and/or mesenchymal properties [52]. Therefore, we propose that in mouse and human mammary glands, *RSPO3* is expressed in the progenitor population promoting their inherent stemness properties and preventing luminal differentiation. Eventually, *RSPO3* overexpression in progenitor cells or expression in the luminal compartment might lead to malignant transformation and transdifferentiation through a process driven by EMT inducers.

Finally, we suggest that RSPO3 might be a potential molecular target for the prevention and treatment of breast cancer, particularly the TN subtype. We hypothesize that blocking its activity might provide a new opportunity not only to reduce tumor bulk but also to deplete CSCs that initiate and promote metastatic spread and recurrence.

Acknowledgements

This project has been supported by grant PICT 2014-0844 awarded by the National Agency of Scientific and Technological Promotion (ANPCyT), Argentina to E.C. Kordon. The authors want to thank Amaranta Avendaño, Lirane Moutinho and Mariela Veggetti for their excellent technical assistance; Mina Bissell, Elisa Bal de Kier Joffé, Laura Todaro and Claudia Lanari for kindly providing cell lines or cell material to develop some of the experiments; Jorge Filmus for providing the pGL3-OT vector, and Ana Quaglino for her guidance in the differentiation assays. J.M.Tocci is indebted to the training provided by Dr. Cathrin Brisken and her team in mouse mammary FACS techniques.

References

[1] de Lau WB, Snel B, Clevers HC. The R-spondin protein family. Genome Biology 2012;13(3).

[2] Kamata T, Katsube K-i, Michikawa M, Yamada M, Takada S, Mizusawa H. R-spondin, a novel gene with thrombospondin type 1 domain, was expressed in the dorsal neural tube and affected in Wnts mutants. Biochimica et Biophysica Acta (BBA) - Gene Structure and Expression 2004;1676(1):51-62.

[3] Kazanskaya O, Glinka A, del Barco Barrantes I, Stannek P, Niehrs C, Wu W. R-Spondin2 is a secreted activator of Wnt/beta-catenin signaling and is required for Xenopus myogenesis. Dev Cell 2004;7(4):525-34.

[4] Ohkawara B, Glinka A, Niehrs C. Rspo3 binds syndecan 4 and induces Wnt/PCP signaling via clathrin-mediated endocytosis to promote morphogenesis. Dev Cell 2011;20(3):303-14.

[5] Carmon KS, Gong X, Lin Q, Thomas A, Liu Q. R-spondins function as ligands of the orphan receptors LGR4 and LGR5 to regulate Wnt/β-catenin signaling. Proceedings of the National Academy of Sciences of the United States of America 2011;108(28):11452–7.

[6] Glinka A, Dolde C, Kirsch N, Huang YL, Kazanskaya O, Ingelfinger D, et al. LGR4 and LGR5 are R-spondin receptors mediating Wnt/beta-catenin and Wnt/PCP signalling. EMBO Rep 2011;12(10):1055-61.

[7] de Lau W, Peng WC, Gros P, Clevers H. The R-spondin/Lgr5/Rnf43 module: regulator of Wnt signal strength. Genes Dev 2014;28(4):305-16.

[8] Clevers H, Nusse R. Wnt/beta-catenin signaling and disease. Cell 2012;149(6):1192-205.

[9] Sternlicht MD. Key stages in mammary gland development: the cues that regulate ductal branching morphogenesis. Breast Cancer Res 2006;8(1):201.

[10] Macias H, Hinck L. Mammary gland development. Wiley interdisciplinary reviews Developmental biology 2012;1(4):533-57.

[11] Zeng YA, Nusse R. Wnt proteins are self-renewing factors for mammary stem cells and promote their long-term expansion in vivo. Cell Stem Cell 2010;6:568-77.

[12] Kordon EC, Smith GH. An entire functional mammary gland may comprise the progeny from a single cell. Development 1998;125(10):1921-30.

[13] Plaks V, Brenot A, Lawson DA, Linnemann JR, Van Kappel EC, Wong KC, et al. Lgr5-expressing cells are sufficient and necessary for postnatal mammary gland organogenesis. Cell Rep 2013;3(1):70-8.

[14] Wang Y, Dong J, Li D, Lai L, Siwko S, Li Y, et al. Lgr4 regulates mammary gland development and stem cell activity through the pluripotency transcription factor Sox2. Stem Cells 2013;31(9):1921-31.

[15] Chu EY, Hens J, Andl T, Kairo A, Yamaguchi TP, Brisken C, et al. Canonical WNT signaling promotes mammary placode development and is essential for initiation of mammary gland morphogenesis. Development 2004;131(19):4819-29.

[16] van Amerongen R, Bowman AN, Nusse R. Developmental stage and time dictate the fate of Wnt/beta-catenin-responsive stem cells in the mammary gland. Cell Stem Cell 2012;11(3):387-400.

[17] Yu QC, Verheyen EM, Zeng YA. Mammary Development and Breast Cancer: A Wnt Perspective. Cancers (Basel) 2016;8(7).

[18] Klauzinska M, Baljinnyam B, Raafat A, Rodriguez-Canales J, Strizzi L, Endo Greer Y, et al. Rspo2/Int7 regulates invasiveness and tumorigenic properties of mammary epithelial cells. Journal of Cellular Physiology 2012;227(5):1960-71.

[19] Seshagiri S, Stawiski EW, Durinck S, Modrusan Z, Storm EE, Conboy CB, et al. Recurrent R-spondin fusions in colon cancer. Nature 2012;488(7413):660-4.

[20] Hao HX, Jiang X, Cong F. Control of Wnt Receptor Turnover by R-spondin-ZNRF3/RNF43 Signaling Module and Its Dysregulation in Cancer. Cancers (Basel) 2016;8(6).

[21] Kazanskaya O, Ohkawara B, Heroult M, Wu W, Maltry N, Augustin HG, et al. The Wnt signaling regulator R-spondin 3 promotes angioblast and vascular development. Development 2008;135(22):3655-64.

[22] Scholz B, Korn C, Wojtarowicz J, Mogler C, Augustin I, Boutros M, et al. Endothelial RSPO3 Controls Vascular Stability and Pruning through Non-canonical WNT/Ca²⁺/NFAT Signaling. Developmental Cell 2016;36(1):79-93.

[23] Kabiri Z, Greicius G, Madan B, Biechele S, Zhong Z, Zaribafzadeh H, et al. Stroma provides an intestinal stem cell niche in the absence of epithelial Wnts. Development 2014;141(11):2206-15.

[24] Gong X, Yi J, Carmon KS, Crumbley CA, Xiong W, Thomas A, et al. Aberrant RSPO3-LGR4 signaling in Keap1-deficient lung adenocarcinomas promotes tumor aggressiveness. Oncogene 2015;34(36):4692-701.

[25] Chartier C, Raval J, Axelrod F, Bond C, Cain J, Dee-Hoskins C, et al. Therapeutic Targeting of Tumor-Derived R-Spondin Attenuates beta-Catenin Signaling and Tumorigenesis in Multiple Cancer Types. Cancer Res 2016.

[26] Gattelli A, Zimberlin MN, Meiss RP, Castilla LH, Kordon EC. Selection of early-occurring mutations dictates hormone-independent progression in mouse mammary tumor lines. J Virol 2006;80(22):11409-15.

[27] Theodorou V, Kimm MA, Boer M, Wessels L, Theelen W, Jonkers J, et al. MMTV insertional mutagenesis identifies genes, gene families and pathways involved in mammary cancer. Nat Genet 2007;39(6):759-69.

[28] Berardi DE, Flumian C, Campodonico PB, Urtreger AJ, Diaz Bessone MI, Motter AN, et al. Myoepithelial and luminal breast cancer cells exhibit different responses to all-trans retinoic acid. Cell Oncol (Dordr) 2015;38(4):289-305.

[29] Prat A, Parker JS, Karginova O, Fan C, Livasy C, Herschkowitz JI, et al. Phenotypic and molecular characterization of the claudin-low intrinsic subtype of breast cancer. Breast Cancer Res 2010;12(5):R68.

[30] Williams C, Helguero L, Edvardsson K, Haldosen LA, Gustafsson JA. Gene expression in murine mammary epithelial stem cell-like cells shows similarities to human breast cancer gene expression. Breast Cancer Res 2009;11(3):R26.

[31] Korkaya H, Paulson A, Charafe-Jauffret E, Ginestier C, Brown M, Dutcher J, et al. Regulation of Mammary Stem/Progenitor Cells by PTEN/Akt/β-Catenin Signaling. PLoS Biol 2009;7(6):e1000121.

[32] Livasy CA, Karaca G, Nanda R, Tretiakova MS, Olopade OI, Moore DT, et al. Phenotypic evaluation of the basal-like subtype of invasive breast carcinoma. Mod Pathol 2006;19(2):264-71.

[33] Recouvreux MS, Grasso EN, Echeverria PC, Rocha-Viegas L, Castilla LH, Schere-Levy C, et al. RUNX1 and FOXP3 interplay regulates expression of breast cancer related genes. Oncotarget 2016;7(6):6552-65.

[34] Blick T, Hugo H, Widodo E, Waltham M, Pinto C, Mani SA, et al. Epithelial Mesenchymal Transition Traits in Human Breast Cancer Cell Lines Parallel the CD44hi/CD24lo/- Stem Cell Phenotype in Human Breast Cancer. Journal of Mammary Gland Biology and Neoplasia 2010;15(2):235-52.

[35] Gilles C, Polette M, Mestdagt M, Nawrocki-Raby B, Ruggeri P, Birembaut P, et al. Transactivation of Vimentin by β-Catenin in Human Breast Cancer Cells. Cancer Research 2003;63(10):2658-64.

[36] Cai C, Yu QC, Jiang W, Liu W, Song W, Yu H, et al. R-spondin1 is a novel hormone mediator for mammary stem cell self-renewal. Genes Dev 2014;28(20):2205-18.

[37] DiMeo TA, Anderson K, Phadke P, Feng C, Perou CM, Naber S, et al. A Novel Lung Metastasis Signature Links Wnt Signaling with Cancer Cell Self-Renewal and Epithelial-Mesenchymal Transition in Basal-like Breast Cancer. Cancer research 2009;69(13):5364-73.

[38] Micalizzi DS, Farabaugh SM, Ford HL. Epithelial-mesenchymal transition in cancer: parallels between normal development and tumor progression. J Mammary Gland Biol Neoplasia 2010;15(2):117-34.

[39] Cichon MA, Nelson CM, Radisky DC. Regulation of Epithelial-Mesenchymal Transition in Breast Cancer Cells by Cell Contact and Adhesion. Cancer Informatics 2015;14(Suppl 3):1-13.

[40] Nelson CM, VanDuijn MM, Inman JL, Fletcher DA, Bissell MJ. Tissue Geometry Determines Sites of Mammary Branching Morphogenesis in Organotypic Cultures. Science 2006;314(5797):298.

[41] Kouros-Mehr H, Werb Z. Candidate regulators of mammary branching morphogenesis identified by genome-wide transcript analysis. Dev Dyn 2006;235(12):3404-12.

[42] Matsuda Y, Schlange T, Oakeley EJ, Boulay A, Hynes NE. WNT signaling enhances breast cancer cell motility and blockade of the WNT pathway by sFRP1 suppresses MDA-MB-231 xenograft growth. Breast Cancer Res 2009;11(3):R32.

[43] Xu J, Prosperi JR, Choudhury N, Olopade OI, Goss KH. beta-Catenin is required for the tumorigenic behavior of triple-negative breast cancer cells. PLoS One 2015;10(2):e0117097.

[44] Constantinou T, Baumann F, Lacher MD, Saurer S, Friis R, Dharmarajan A. SFRP-4 abrogates Wnt-3a-induced β-catenin and Akt/PKB signalling and reverses a Wnt-3a-imposed inhibition of in vitro mammary differentiation. Journal of Molecular Signaling 2008;3:10-.

[45] Zhang M, Atkinson RL, Rosen JM. Selective targeting of radiation-resistant tumor-initiating cells. Proceedings of the National Academy of Sciences of the United States of America 2010;107(8):3522-7.

[46] Creighton CJ, Li X, Landis M, Dixon JM, Neumeister VM, Sjolund A, et al. Residual breast cancers after conventional therapy display mesenchymal as well as tumor-initiating features. Proc Natl Acad Sci U S A 2009;106(33):13820-5.

[47] Vadnais C, Shooshtarizadeh P, Rajadurai CV, Lesurf R, Hulea L, Davoudi S, et al. Autocrine Activation of the Wnt/beta-Catenin Pathway by CUX1 and GLIS1 in Breast Cancers. Biology open 2014;3(10):937-46.

[48] Khramtsov AI, Khramtsova GF, Tretiakova M, Huo D, Olopade OI, Goss KH. Wnt/β-Catenin Pathway Activation Is Enriched in Basal-Like Breast Cancers and Predicts Poor Outcome. The American Journal of Pathology 2010;176(6):2911-20.

[49] López-Knowles E, Zardawi SJ, McNeil CM, Millar EKA, Crea P, Musgrove EA, et al. Cytoplasmic Localization of β-Catenin is a Marker of Poor Outcome in Breast Cancer Patients. Cancer Epidemiology Biomarkers & Prevention 2010;19(1):301-9.

[50] Geyer FC, Lacroix-Triki M, Savage K, Arnedos M, Lambros MB, MacKay A, et al. beta-Catenin pathway activation in breast cancer is associated with triple-negative phenotype but not with CTNNB1 mutation. Mod Pathol 2011;24(2):209-31.

[51] Rooney N, Riggio AI, Mendoza-Villanueva D, Shore P, Cameron ER, Blyth K. Runx Genes in Breast Cancer and the Mammary Lineage. In: Groner Y, Ito Y, Liu P, Neil JC, Speck NA, van Wijnen A, editors. RUNX Proteins in Development and Cancer. Singapore: Springer Singapore; 2017, p. 353-68.

[52] Pfefferle AD, Spike BT, Wahl GM, Perou CM. Luminal progenitor and fetal mammary stem cell expression features predict breast tumor response to neoadjuvant chemotherapy. Breast Cancer Research and Treatment 2015;149:425-37.

Figure legends

Figure 1. *RSPO3* is expressed in human and mouse mammary cancer cell lines. (A) *RSPO3* mRNA expression profile based on a compiled *in silico* dataset of 50 human breast cancer cell lines (BCCLs): 27 luminal-like and 23 basal-like BCCLs, and the non-tumorigenic MCF-10A cell line, obtained from GSE10843, GSE12777, and GSE41445 datasets. (B) Box plot of *RSPO3* mRNA expression between non-tumor, luminal-like and basal-like BCCLs from the compiled dataset, showing statistically significant differences between groups. (C) Hierarchical clustering analysis and (D) correlation matrix of *RSPO3, CDH1*, *VIM*, *FN1*, *SNAI1*, *SNAI2*, and *TWIST* among breast cancer cell lines using the same datasets as in A. Green squares in (D) show genes with statistically significant differences; p<0.01. (E) Reverse Transcription-quantitative PCR (RT-qPCR) analysis of *Rspo3* mRNA expression levels and the basal/mesenchymal marker vimentin (*Vim*) in tumor (LM38-LP, SCg6, C4-L2, C4-HI, C4HD and C4-HIR) and non-tumor (HC11, SCp2 and EpH4) mouse mammary cells. Analysis of *Rspo3* expression in HC11 cells was performed during proliferative stem-like (HC11-P) and lactogenic differentiation (HC11-D) stages. Expression data were normalized by *HSP90ab1* mRNA and error bars are s.e.m. (n=3). (F) Representative Western blot (WB) analysis of RSPO3 levels in serum-free conditioned media (CM) and total cell lysates (TCLs) of indicated mouse mammary cell lines. LM3: ER^-PR^- mouse mammary tumor cell line. Cells were cultured in serum-free medium for 24 or 48 h prior to harvesting. β-actin was used as a loading control. (G) Representative WB analysis of RSPO3 levels in TCL and serum-free CM of SCg6 cells incubated with increasing concentrations (0-25 mM) of potassium chlorate ($KClO_3$), an inhibitor of sulfation. β-actin was used as a loading control. * high molecular weight band of RSPO3, possibly due to post-translational modifications.

Figure 2. *Rspo3* is expressed in the stroma and stem cell-enriched basal mammary epithelial cell subpopulations. (A) Immunohistochemical staining of serial mouse mammary sections with antibodies specific to RSPO3 and to stem (SOX2), basal (Cytokeratin14, KRT14, and α-SMA), and luminal (ERα) lineage markers. Lower panels correspond to higher magnification of upper images. Scale bars: 50 µm and 17 µm, respectively. (B) Representative micrographs of co-immunofluorescence assays showing RSPO3 (red), α-SMA (green, upper panels), and ERα (green, lower panels), in mouse mammary sections; DAPI (blue) shows nuclei. Scale bars: 50 µm. (C) FACS segregation of lineage-negative (Lin: CD31, CD45, Ter119) mammary cells into luminal ($CD24^{hi}CD29^+$), stem cell-enriched basal ($CD24^+CD29^{hi}$) and stromal ($CD24^-CD29^+$) subpopulations. A representative FACS dot plot is shown. (D) RT-qPCR analysis of luminal Cytokeratin 18 (*Krt18*), basal *Krt14*, stem *Lgr4*, mesenchymal *Vim* markers, and *Rspo3* expression in luminal, basal/stem and stromal FACS-sorted subpopulations normalized to *HSP90ab1*. Data represent mean +/- s.e.m. of three replicate experiments; Tukey´s test following one-way ANOVA. *, **, *** P<0.05; n.s. not-significant. All experiments were performed using 12-week-old virgin female mice.

Figure 3. RSPO3 inhibits lactogenic differentiation and promotes mesenchymal/basal phenotype in mouse mammary epithelial cells. (A) *Rspo3* mRNA expression determined by oligo-microarray analysis (probe 1443187_at) obtained from GSE47377 GEO Superserie of alveolar epithelial cells: luminal progenitors (LP) and luminal mature at mid-gestation (LM), isolated from the mammary glands of adult virgin female mice. (B) Quantitative expression analysis of β-casein gene. Mouse mammary luminal-like SCp2 and EpH4 cells were cultured in the presence of lactogenic hormones, with or without 1.5% v/v laminin-rich basement membrane (Matrigel) to promote lactogenic differentiation, and with or without rRSPO3 (60 ng/ml) for 72 h. Total RNA was isolated and subjected to RT-qPCR. (C) Representative micrographs showing morphological changes induced in NMuMG cells 24 h after treatment with rRSPO3 protein (60 ng/ml) or TGF-β (2 ng/ml) as an EMT-positive control. (D) RT-qPCR analysis of mesenchymal (vimentin and fibronectin) and epithelial (E-cadherin) markers in NMuMG

cells treated or not with rRSPO3 protein during 24 and 72 h. Gene expression data were normalized to *HSP90ab1* mRNA and is shown as fold change (mean +/- s.e.m.) relative to untreated cells. (E) Representative WB analysis of EMT-associated markers in NMuMG cells 24 h and 72 h after treatment with rRSPO3. β-actin was used as a loading control. Experiments B-E were performed in triplicate. Student´s t-test, *: P<0.05; n.s. not significant.

Figure 4. *Rspo3* down-regulation alters basal phenotype in tumor SCg6 mammary cells. (A) WB analysis of RSPO3 levels in SCg6 cells either naïve (Parental), or stably transfected with a scrambled shRNA (shControl) or with shRNA sequences targeting *Rspo3* (shRspo3). 2A and 4B represent two different isolated clones. (B) Representative micrographs of confluent shRspo3-2A and 4B, and shControl cells. Original magnification: 200x. (C) and (D) Representative micrographs of immunocytochemistry assays showing F-actin (red) and β-catenin (red), respectively, in stably transfected shRspo3 (clone 4B) or shControl SCg6 cells; DAPI (blue) shows nuclei. Scale bars: 10 µm. (E) RT-qPCR analysis of basal/mesenchymal markers, vimentin and fibronectin, in shRspo3 and shControl cells. Gene expression data were normalized to *HSP90ab1* mRNA and are shown as fold change (mean +/- s.e.m.) relative to shControl cells. Experiments were performed in triplicate and Dunnett´s test following one-way ANOVA was performed. *: P<0.05. (F) Representative micrographs of immunocytochemistry assays showing vimentin (red, upper panels) and fibronectin (red, lower panels) in stably transfected shRspo3 (clone 4B) or shControl SCg6 cells; DAPI (blue) shows nuclei. (G) Representative images of wound healing assays performed with SCg6 cells, with a graph showing the quantitation of cell migration (n=4; *P<0.05 indicates statistically significant differences vs. shControl migration; Dunnett´s test following one-way ANOVA). (H) shRspo3 and shControl cells were transiently transfected with Luciferase β-catenin reporter and β-galactosidase (normalizing transfection control) vectors. The reporter activity was measured 48 h after transfection. Error bars represent the s.d. (n=4). Student´s t-test, *P<0.05.

Figure 5. *Rspo3* down-regulation in SCg6 cells reduces tumor growth and metastasis *in vivo*. (A) Tumor growth of shRspo3 (clone: 4B) and shControl cells implanted subcutaneously. Tumors were measured with a caliper starting at 9 d after inoculation, when the tumors became detectable under the skin. Their volumes were calculated using the formula $\pi/6 \times a \times b^2$, where *a* is the longest dimension of the tumor, and b is the width. (B) Representative image of intra-mammary shRspo3-4B and shControl tumors isolated from mice 20 days post-injection (scale bar: 50 mm). (C) Tumor growth of shRspo3 (clone: 4B) and shControl cells implanted into #4 mammary fat pad (day=0) BALB/c females. (D) Representative micrographs showing H&E (OM: 100x) and RSPO3, vimentin, Ki67 and cleaved-caspase 3 (CC3) IHC (OM: 400x) in shRspo3-4B and shControl tumors obtained after cell inoculation into cleared-fat pads. Arrowheads point to CC3 positive cells. Quantification of Ki67 and CC3 positive cells is shown in lower graphs. Student´s t-test, *P<0.05. (E) Representative image and macrometastasis quantification of excised lungs 30 days after tail vein inoculation of shRspo3-4B and shControl cells. n=3. (F) Representative micrographs of H&E staining of lung tissue invaded by shRspo3-4B and shControl cells, 15 or 30 days after cell injection into the tail vein. *: mammary tumor cells; OM: 100x. (G) Metastasis quantification by lung metastasis area index, 30 days after cell inoculation; n=3. H&E: Hematoxylin and Eosin staining, OM: Original Magnification, IHC: immunohistochemistry.

Figure 6. *RSPO3* is expressed in human breast cancer and in the basal compartment of non-neoplastic breast tissue. IHC studies were carried out on several breast samples. (A) Lobular carcinoma *in situ* (LCIS) and stromal infiltrating cells (arrows) with moderate immunostaining and a small duct (arrowhead) with strong immunostaining for RSPO3. (B) Infiltrating cords (arrows) of a ductal not otherwise specified (NOS) carcinoma with moderate immunostaining for RSPO3. (C) Intense cytoplasmic immunostaining for RSPO3 in cells (arrows) of a ductal NOS carcinoma. (D) Rows of infiltrating cells from a lobular carcinoma, some with moderate (arrows) and

others with negative (arrowhead) immunostaining for RSPO3. Original magnification of A-D: 400x. (E-H) Representative micrographs showing intense RSPO3 immunostaining in basal and myoepithelial cells of lobules and ducts from human hyperplastic breast sections; scale bar of left panels: 50 µm; scale bars of right panels: 100 µm. Original magnification of E-H: 400x. (I-N) Representative tissue microarray micrographs of ductal invasive breast carcinoma samples showing infiltrating cords with cytoplasmic negative (I-J), low/moderate (K-L) or strong (M-N) RSPO3 immunostaining. In (J) tumor tissue is surrounded by positive lymphocytes and fibroblasts. In (M) some cells display a perinuclear reinforcement of RSPO3 expression. Original magnification of I-M: 400x. Percentages of cases with negative, low/moderate and strong RSPO3 immunostaining are indicated for each of these categories.

Figure 7. Basal-like breast tumors show high expression of *RSPO3.* (A) *RSPO3* expression levels according to ER, PR, and Her2 biomarker expression using *in silico* data mining of the TCGA cBioportal METABRIC database (1985 samples). $ER^-PR^-Her2^-$ vs: $ER^-PR^-Her2^+$, $ER^-PR^+Her2^-$ or $ER^-PR^+Her2^+$ resulted not significant by Pairwise comparisons using Tukey and Kramer test. (B) Comparative box plot analysis of *RSPO3* mRNA expression profiles according to intrinsic subtypes (luminal A, luminal B, Her2, and basal-like) among primary breast carcinomas, by Pairwise comparisons using Tukey and Kramer test and the same TCGA's dataset as in A. Correlation analysis among normal and breast cancer samples was done using R/Bioconductor software. (C) Comparative box plot analysis of *RSPO3* mRNA expression, according to intrinsic breast cancer subtypes, separating claudin-low subtype from basal-like category using the same TCGA's dataset as in A. (D) Box plot expression analysis of *RSPO3* with respect to expression level of *CDH1* (E-cadherin), *VIM* (vimentin), *SNAI2* (Slug), and *TWIST*, as EMT markers, using the same TCGA's dataset as in A. Kruskal-Wallis chi-squared was used as statistic test. (E) Box plot of *RSPO3* mRNA expression in association with stromal and immune scores using the ESTIMATE method in the TCGA-Breast cancer RNA-Seq dataset (1097 primary breast carcinomas samples) obtained from UCSC Xena Browser (https://xenabrowser.net). *RSPO3* mRNA expression was classified in high or low levels based on StepMiner one-step algorithm. (F) *RSPO3* mRNA levels in association with negative/low or moderate/high *LGR4-6* expression levels among the TCGA-Breast cancer RNA-Seq dataset as in E. (G) Correlation analysis of *RSPO3* expression with mRNA levels of its putative receptors, *LGR4-6*, and a member of the transcription factor family of *RUNX* genes, *RUNX3*, in human breast samples using the TCGA-Breast cancer RNA-Seq dataset as in E. (H) *LGR4-6* and *RUNX3* expression levels among the intrinsic breast cancer subtypes based on gene expression profiling, using the same the TCGA-Breast cancer RNA-Seq dataset as in E.

Figure 1

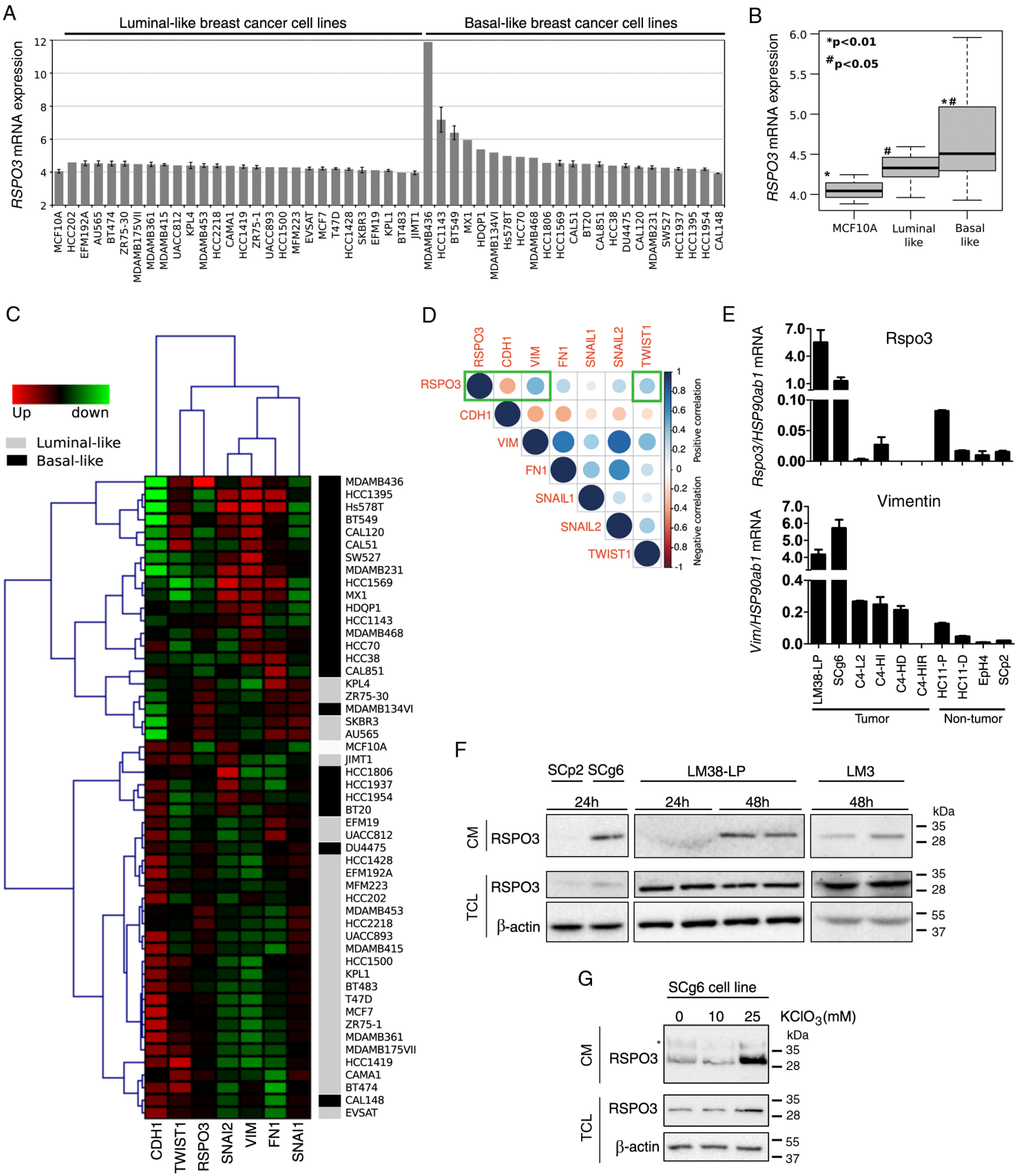

Figure 2

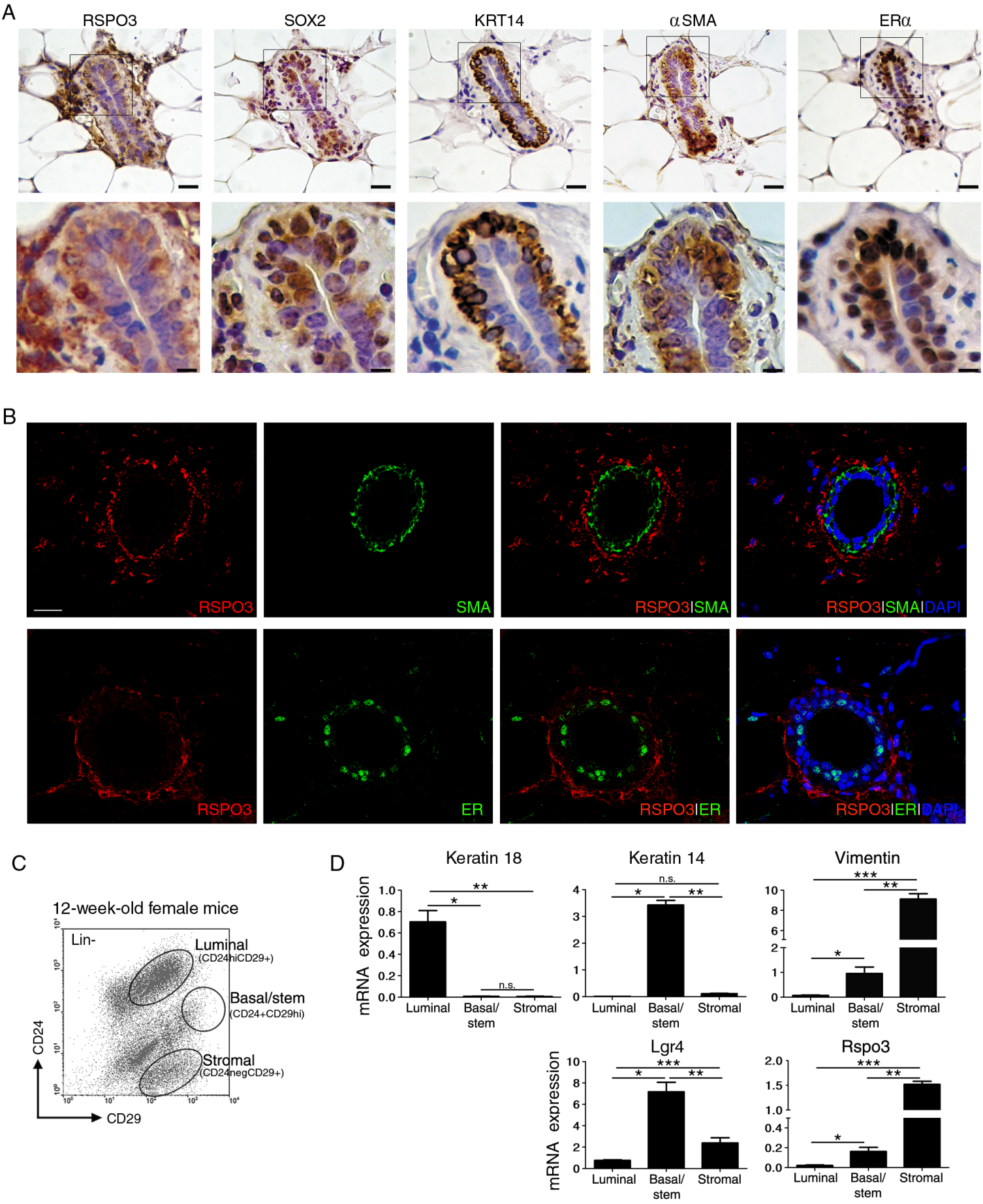

Figure 3

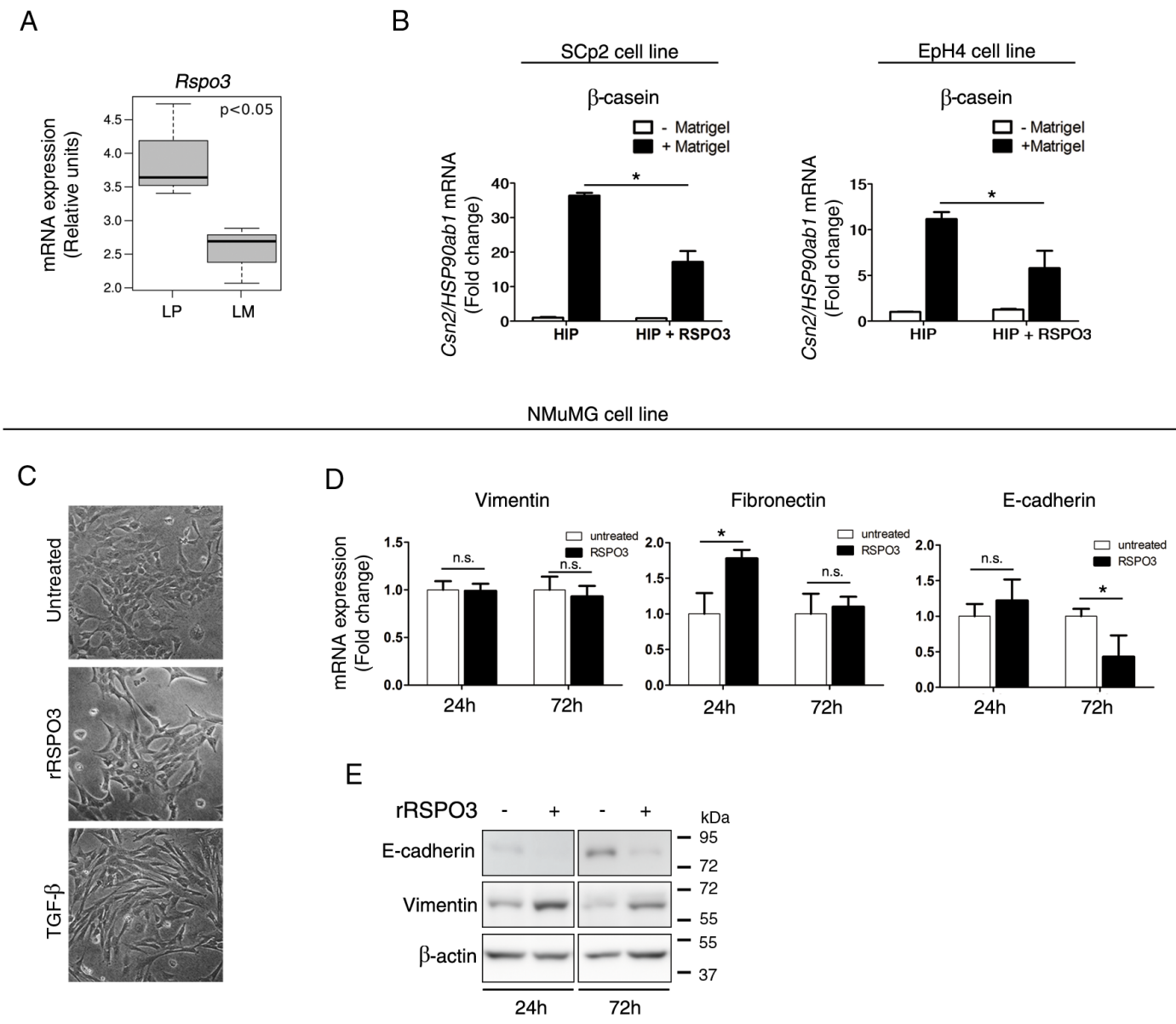

Figure 4

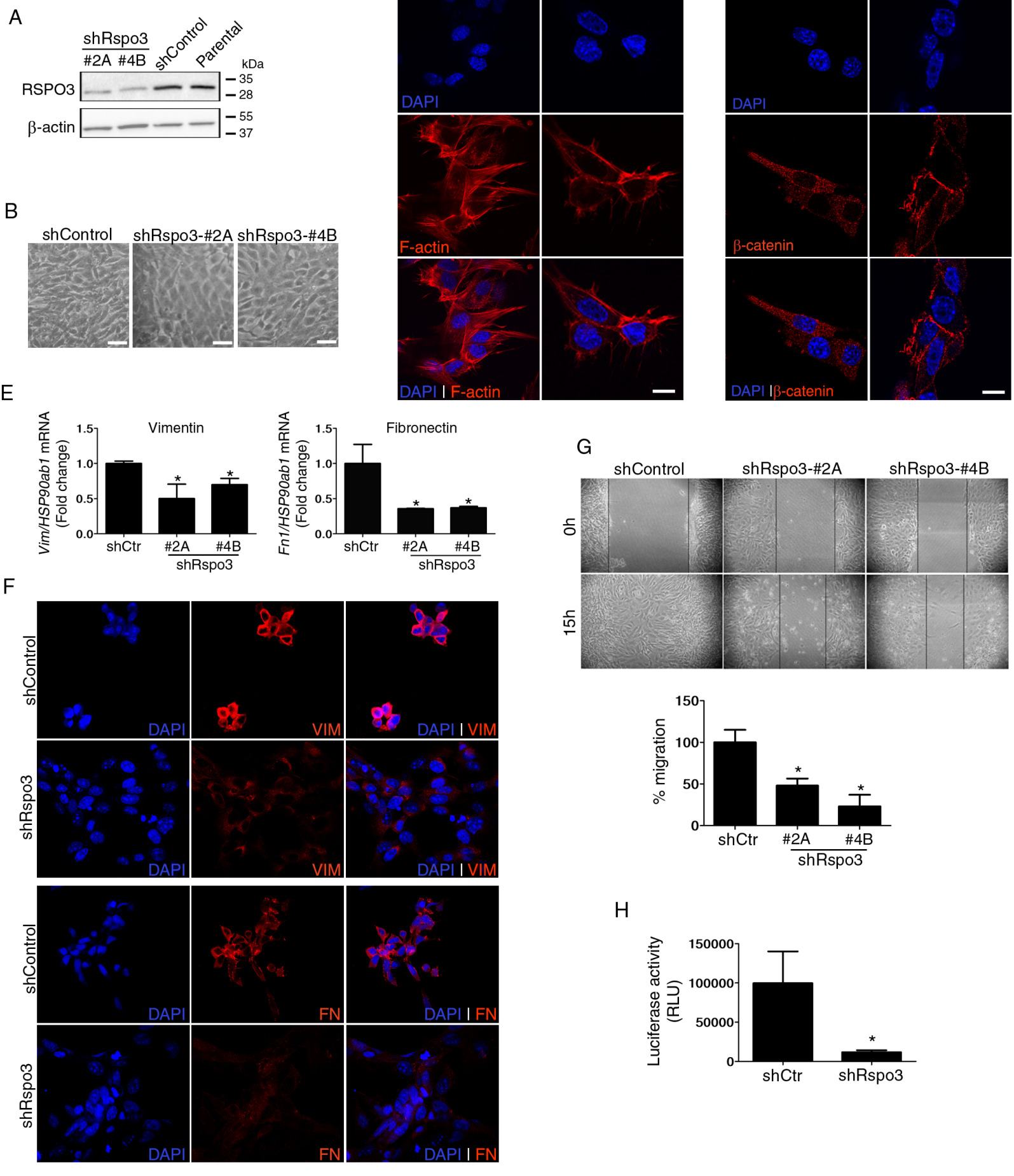

Figure 5

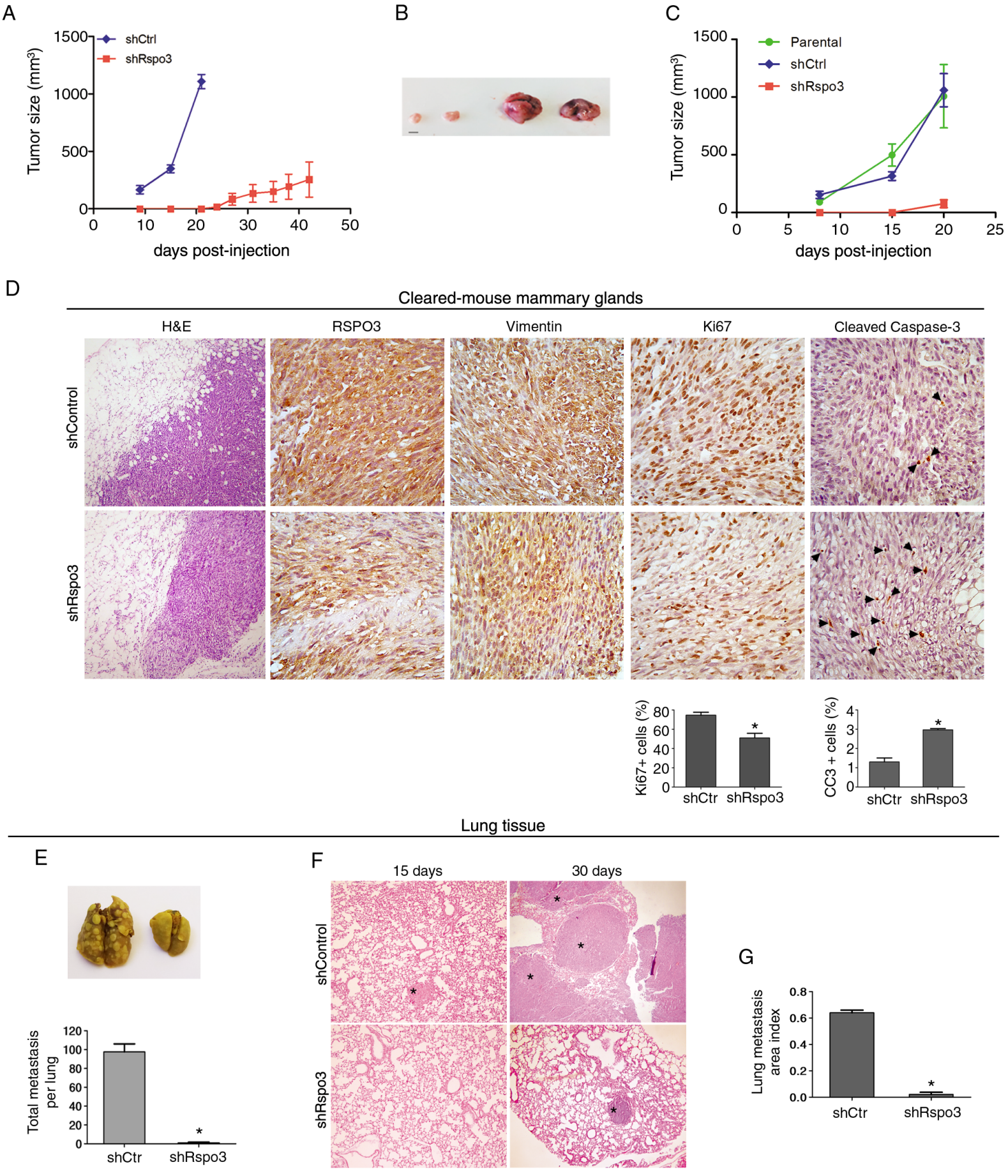

Figure 6

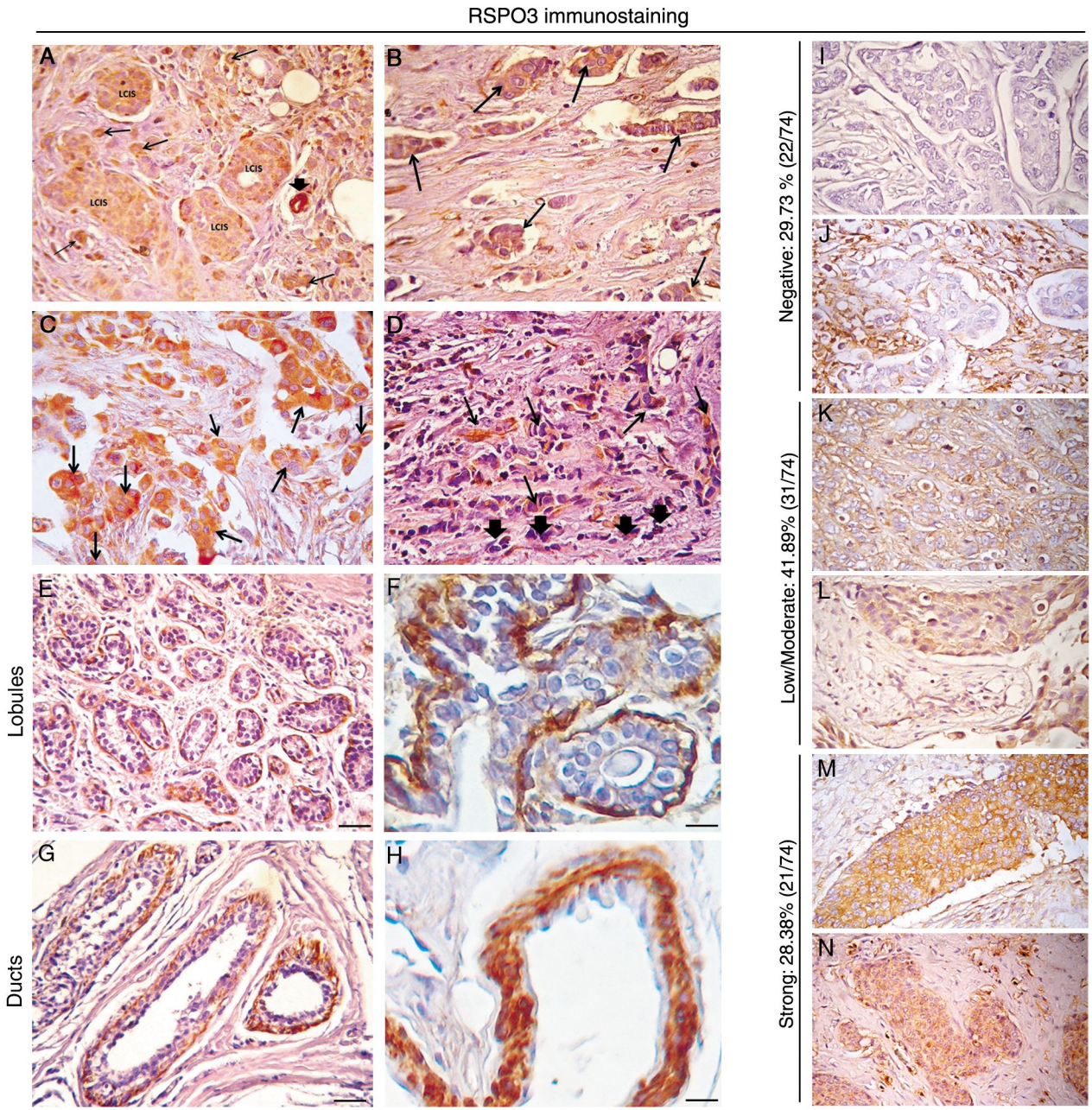

Figure 7

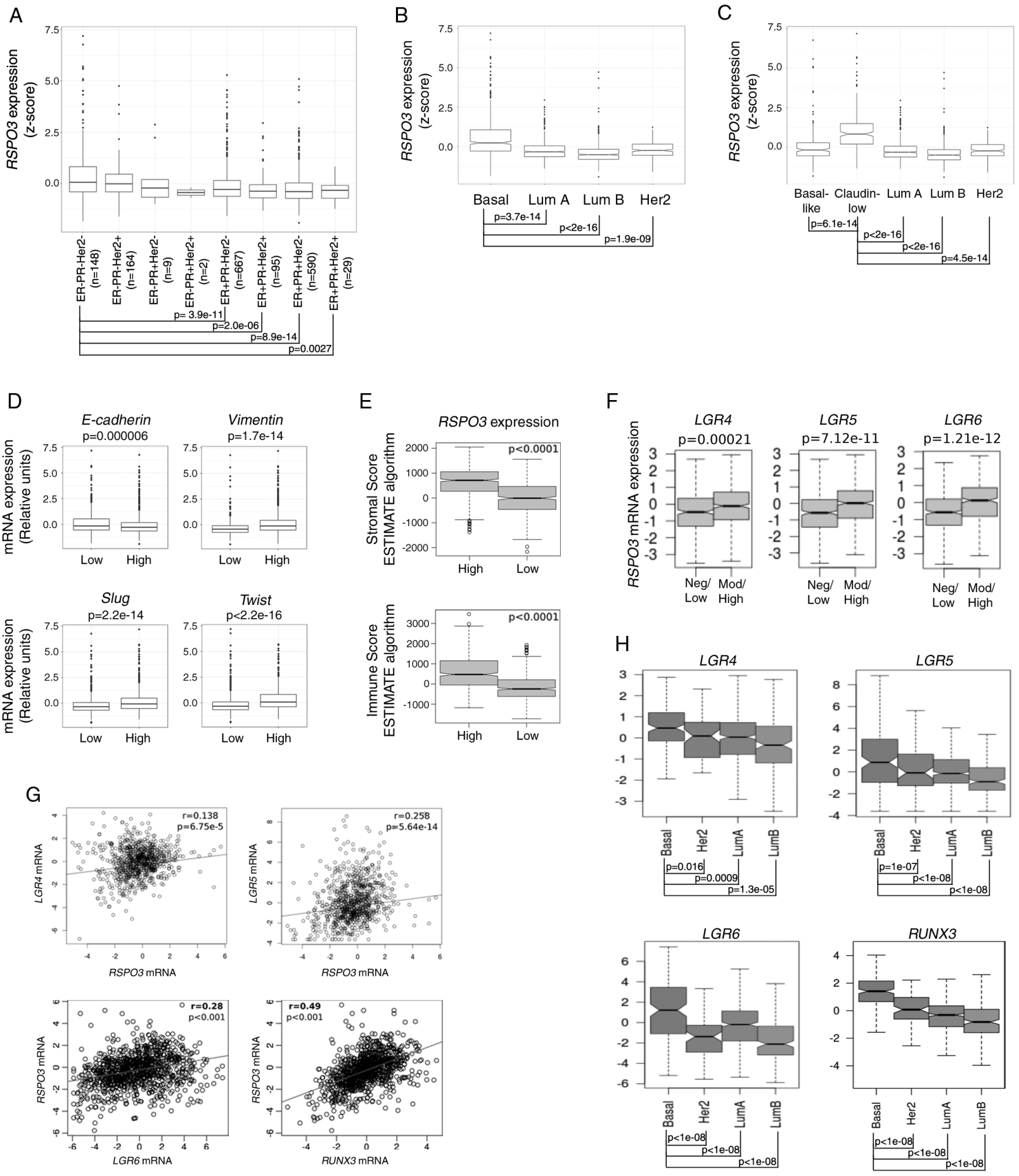

Cancer Research
The Journal of Cancer Research (1916–1930) | The American Journal of Cancer (1931–1940)

AACR American Association for Cancer Research

R-spondin3 is associated with basal-progenitor behavior in normal and tumor mammary cells

Johanna Melisa Tocci, Carla María Felcher, Martín E García Solá, et al.

Cancer Res Published OnlineFirst May 10, 2018.